

Cuprates phase diagram deduced from magnetic susceptibility : what is the ‘true’ pseudogap line ?

Yves Noat,¹ Alain Mauger,² Minoru Nohara,³ Hiroshi Eisaki,⁴ Shigeeyuki Ishida,⁴ and William Sacks²

¹*Institut des Nanosciences de Paris, CNRS, UMR 7588*

Sorbonne Université, Faculté des Sciences et Ingénierie, 4 place Jussieu, 75005 Paris, France

²*Institut de Minéralogie, de Physique des Matériaux et de Cosmochimie, CNRS, UMR 7590,*

Sorbonne Université, Faculté des Sciences et Ingénierie, 4 place Jussieu, 75005 Paris, France

³*Department of Quantum Matter, Hiroshima University,*

1-3-1 Kagamiyama, Higashi-Hiroshima, Japan 739-8530

⁴*Research Institute for Advanced Electronics and Photonics (RIAEP),*

National Institute of Advanced Industrial Science and Technology (AIST), Tsukuba, Ibaraki 305-8568, Japan

(Dated: 8 février 2022)

Two contradictory phase diagrams have dominated the literature of high- T_c cuprate superconductors. Does the pseudogap line cross the superconducting T_c -dome or not? To answer, we have revisited the experimental magnetic susceptibility and knight shift of four different compounds, $\text{La}_{1-x}\text{Sr}_x\text{CuO}_4$, $\text{Bi}_2\text{Sr}_2\text{Ca}_{1-x}\text{Y}_x\text{Cu}_2\text{O}_8$, $\text{Bi}_2\text{Sr}_2\text{CaCu}_2\text{O}_{8+y}$, $\text{YBa}_2\text{Cu}_3\text{O}_{6+y}$, as a function of temperature and doping. The susceptibility can be described by the same function for all materials, having a magnetic and an electronic contributions. The former is the 2D antiferromagnetic (AF) square lattice response, with a characteristic temperature of magnetic correlations T_{max} . The latter is the ‘Pauli’ term, revealing the gap opening in the electronic density of states at the pseudogap temperature T^* .

From precise fits of the data, we find that $T_{max}(p)$ decreases linearly as a function of doping (p) over a wide range, but saturates abruptly in the overdoped regime. Concomitantly, $T^*(p)$ is *linear and tangent* to the dome, either crossing or approaching $T_{max}(p)$ at the top of the dome, indicating a qualitative change of behavior from underdoped to overdoped regimes.

Contrary to the idea that the pseudogap terminates just above optimal doping, our analysis suggests that the gap exists throughout the phase diagram. It is consistent with a pseudogap due to hole pairs, or ‘pairs’, above T_c . We conclude that T_{max} , reflecting the AF magnetic correlations, has often been misinterpreted as the pseudogap temperature T^* .

PACS numbers: 74.72.h, 74.20.Mn, 74.20.Fg

Introduction

Since the discovery of cuprates by Bednorz, and Müller [1] in 1986, the phase diagram of high- T_c superconductors remains a puzzle. In the underdoped regime a gap persists at the Fermi level above the critical temperature, called the pseudogap (PG) (see Ref. [2] for a review). First discovered by NMR [3, 4], it was rapidly confirmed by optical conductivity [5, 6], neutron scattering [7, 8], transport [9–12], specific heat [13], tunneling [14, 15] and photoemission spectroscopies [16, 17].

The pseudogap is one of the key ingredients distinguishing high- T_c cuprates from conventional superconductors, which are successfully described by the Bardeen-Cooper-Schrieffer (BCS) theory [18]. Indeed, BCS superconductors are characterized by a gap in the quasiparticle excitation spectrum that closes at the critical temperature concomitantly with the disappearance of superconducting coherence.

While the existence of a pseudogap phase above T_c is well established, its relationship to the superconducting state is still strongly debated, as discussed in detail by Kordyuk in Ref. [19]. Two main avenues have emerged in the literature to understand this issue :

i) The pseudogap is a precursor of superconductivity,

with incoherent preformed pairs existing above T_c .

ii) The pseudogap is linked to a competing order such as a spin density wave or charge order.

According to the hypothesis (i), the pseudogap exists for any doping value in the range where T_c does not vanish, while according to (ii), the pseudogap exists only below some lower critical value of the hole concentration. In order to address this unresolved issue, it is crucial to know the temperature at which the gap in the electronic density of states (DOS) opens, as a function of carrier concentration.

We define T^* , and maintain this definition throughout, as the temperature at which a quasiparticle gap at the antinodal point $(0, \pi)$ in angle-resolved photoemission spectroscopy (ARPES) or a gap at the Fermi level in tunneling, vanishes with rising temperature. The PG temperature T^* can be measured *directly* by electronic spectroscopic probes, such as tunneling or photoemission spectroscopies (see Ref. [20] and [21] for comprehensive reviews), but only *indirectly* through the resistivity, specific heat or magnetic susceptibility. In the latter cases, the determination of T^* can be complex, as we shall discuss in this paper for the magnetic susceptibility, since the gap in the electronic DOS must be inferred using an appropriate theory.

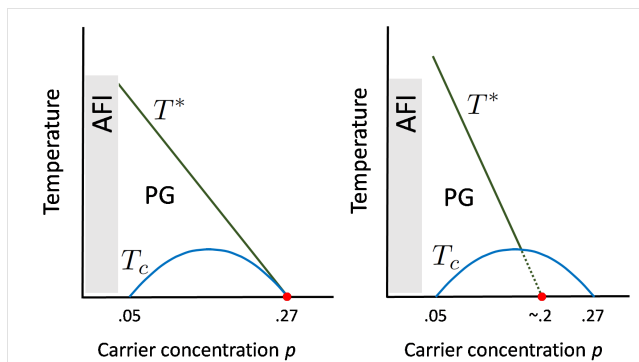


FIGURE 1. (Color online) Schematic of the two generic phase diagrams : Left panel : A pseudogap exists for all doping and ending at the maximum doping $p_c = 0.27$. This phase diagram is generally deduced from direct probes such as tunneling and photoemission spectroscopy. Right panel : The pseudogap line crosses the superconducting dome, ending at the critical doping $p_c \approx 0.2$. This class of phase diagrams is generally deduced from indirect probes, such as transport, specific heat or magnetic susceptibility measurements.

Based on the wide variety of measurements mentioned above, two general classes of phase diagrams are readily encountered in the literature (see figure 1), each of them in favor of one of the two hypotheses mentioned above. In the first class (Fig. 1, left panel), the pseudogap exists for any doping along the superconducting dome [22], where the $T^*(p)$ line arrives tangential to the dome. In an alternative phase diagram (Fig. 1, right panel), the pseudogap is suggested to terminate near the top of the dome or inside the dome [23–25], at a critical value associated with a quantum critical point (see [26] and Ref. therein).

Not only is there a quantitative difference between the two phase diagrams but also a qualitative one : Indeed, using ARPES, several teams have shown the existence of the pseudogap in the DOS above T_c in the overdoped regime, at least up to $p = 0.2$ [27, 28] whereas Loram et al. and Naqib et al. report a pseudogap deduced from the magnetic susceptibility [29, 30], the resistivity [24] and the specific heat [31, 32], vanishing at $p = 0.19$.

In this article, we revisit the magnetic susceptibility of high- T_c cuprates and show that a proper analysis allows to reconcile the contradictory phase diagrams of the literature. Our results show that there is not one, but *two* characteristic temperatures present in the phase diagram. The first one is T^* , unambiguously defined as the temperature at which a gap in the electronic DOS opens at the Fermi level in the antinodal direction. The second is T_{max} , the characteristic temperature of 2D antiferromagnetic correlations. It is defined experimentally as the temperature of the maximum in the magnetic susceptibility.

Our analysis points to a the pseudogap in the DOS, following T^* , existing for all doping values along the superconducting dome. The temperature dependence of the

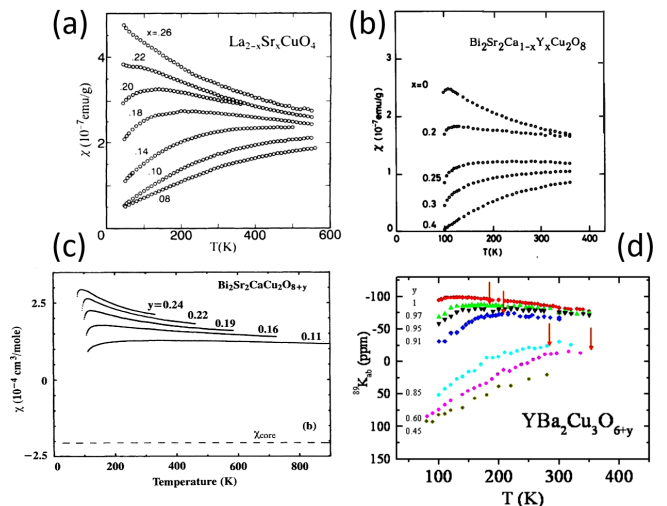


FIGURE 2. (Color online) Experimental susceptibility as function of temperature and doping measured for different materials in the cuprate family : a) $\text{La}_{2-x}\text{Sr}_x\text{CuO}_4$ by Nakano et al. [46], b) $\text{Bi}_2\text{Sr}_2\text{Ca}_{1-x}\text{Y}_x\text{Cu}_2\text{O}_8$ by Oda et al. [47], c) $\text{Bi}_2\text{Sr}_2\text{CaCu}_2\text{O}_{8+y}$ by Allgeier et al. [48] d) Knight shift measured in $\text{YBa}_2\text{Cu}_3\text{O}_{6+y}$ by Alloul et al. [49].

DOS is due to the excitation of hole pairs or pairons [33, 34] above T_c , and their dissociation into quasiparticles [35, 36]. The ‘so-called’ pseudogap deduced in previous works from the magnetic susceptibility [29, 30, 37] is in fact T_{max} , the characteristic temperature of magnetic correlations. It is clearly distinct from T^* , that is the onset temperature of a gap in the electronic DOS at the Fermi level. While both temperatures depend on a unique energy scale, the exchange energy J , we show in this paper that they are not simply proportional, as suggested in Ref. [38].

Magnetic susceptibility of high- T_c cuprates

The magnetic susceptibility $\chi(T)$ of cuprates has been extensively studied as function of temperature and doping for different materials [39–45]. We have chosen representative materials and measurements with a wide doping range. We have focused attention on $\text{La}_{1-x}\text{Sr}_x\text{CuO}_4$ (LSCO) by Nakano et al. [46], Y-doped $\text{Bi}_2\text{Sr}_2\text{Ca}_{1-x}\text{Y}_x\text{Cu}_2\text{O}_8$ (Y-BSCCO) by Oda et al. [47], oxygen doped $\text{Bi}_2\text{Sr}_2\text{CaCu}_2\text{O}_{8+y}$ (BSCCO) by Allgeier et al. [48]. We have also analyzed the Knight shift measured in $\text{YBa}_2\text{Cu}_3\text{O}_{6+y}$ (YBCO) by Alloul et al. [49], (see Fig.2).

Clearly, even before a detailed analysis, one observes similar trends in the data : at low hole doping, i.e. in the underdoped regime, $\chi(T)$ is a smooth increasing function of temperature. However, at intermediate doping, i.e. close to the optimal doping value $p = 0.16$, $\chi(T)$ de-

velops a pronounced maximum at a characteristic temperature, which is followed by a power law decay. This maximum monotonically decreases towards T_c in the overdoped regime.

In the underdoped case, where the susceptibility increases with temperature, it is tempting to offer an immediate explanation based on the electronic DOS. Since in a metal the electronic Pauli susceptibility is independent of temperature, one tempting interpretation is to attribute this behavior to a gap in the electronic DOS above T_c . In this approach, a pseudogap would exist in the doping range where the susceptibility decreases upon cooling, i.e. roughly below optimal doping.

This is the spirit of the work of Naqib et al., who report in several articles the measurement of the magnetic susceptibility as function of temperature and doping in LSCO and YBCO [29, 30]. To analyse their data, they assumed that $\chi(T)$ is essentially due to the temperature dependence of the electronic DOS at the Fermi level. The reduction of $\chi(T)$ observed at low temperature in the underdoped regime was then explained using a temperature-independent gap at the Fermi level. The temperature dependence of $\chi(T)$ was then attributed to the thermal electron-hole excitations through this gap, like in any semiconductor.

From the fit of their data, they deduced an energy gap E_g that varies linearly with p , vanishing at a critical value $p = 0.19$. Their approach provides a satisfactory explanation for YBCO, given the good quality of the fits. Their temperature scale E_g/k_B gives a phase diagram belonging to the class of Fig. 1, right panel.

However, the approach no longer works for LSCO, since for intermediate hole doping, the susceptibility $\chi(T)$ develops a maximum, followed by a power law decrease as a function of temperature. Moreover, as in a more recent paper [50], the gap energy E_g shows no sign of closing up to high temperatures ($T \sim 400K$), but such a rigid gap is difficult to justify in a metallic system. Moreover, above optimum doping, the concave nature of $\chi(T)$ becomes even more pronounced and its shape as a function temperature can no longer be described by a gap in the electronic DOS.

Contribution of the AF 2D lattice to the susceptibility

In this paper we take a different approach that overcomes these discrepancies and gives an accurate description of the magnetic susceptibility. It includes the magnetic contribution of the 2D lattice which has been very well established in the literature of cuprates in the 1990's. Indeed, the overall shape of the magnetic susceptibility has been convincingly attributed to the response of the AF CuO planes, not included by Naqib et al. [29, 30].

In a pioneering work, Johnston [39] has shown that

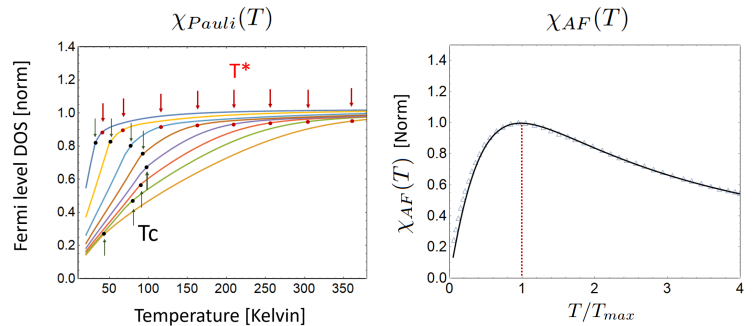


FIGURE 3. (Color online) a) Temperature dependent density of states at the Fermi level for different hole doping, calculated in the pairon model. It takes into account the convolution with the Fermi-Dirac distribution, as in formula 9. b) Magnetic contribution of the susceptibility using equation 2, solid line. Open triangles : results of Nakano et al. in $\text{La}_{1-x}\text{Sr}_x\text{CuO}_4$ [46], showing a perfect match.

the magnetic susceptibility in LSCO is dominated by the magnetic contribution of the CuO square lattice. This approach was extensively revisited by Nakano et al. [46] and independently by other authors [45, 48]. In particular, the magnetic response of a 2D Heisenberg antiferromagnetic square lattice has been calculated in the literature. Given the Heisenberg Hamiltonian $H = \sum_{i,j} JS_i \cdot S_j$, where the sum runs over all pairs of nearest neighbors i and j , the general form for the susceptibility of the 2D AF square lattice is given by Lines [51] :

$$\frac{Ng^2\mu_b^2}{\chi(T)J} = 3\vartheta + \sum_{n=1}^{\infty} \frac{C_n}{\vartheta^{n-1}} \quad (1)$$

where $\vartheta = k_B T / [JS(S+1)]$ with k_B being the Boltzmann constant, N the number of spins, g the Landé g -factor, μ_B the Bohr magneton. The coefficients C_n in the series of Eq. 1 are known and tabulated in Ref. [51] for different spin value.

Although Eq. 1 was rigorously established for the undoped 2D square lattice, we found that the magnetic part of the doped system is satisfactorily described by the first two terms of the sum in Eq. 1, leading to :

$$\chi_{AF}(T) = A_{mag} \left(T + \frac{T_{max}^2}{T} + C \right)^{-1} \quad (2)$$

where A_{mag} , T_{max} and C are doping-dependent parameters. The magnetic part of the susceptibility gives a universal curve (see Fig. 3, right panel), having a peak at $T = T_{max}$, the characteristic scale of AF correlations, and a $\chi_{AF}(T) \sim A_{mag}/(T + C)$ Curie or Curie-Weiss behavior at high temperature (i.e. for $T \gg T_{max}$). Note that T_{max} plays a central role since it reflects the characteristic temperature below which magnetic correlations are important.

In a first approach, one reproduces the measured magnetic susceptibility in LSCO (Fig. 2a) by assuming that

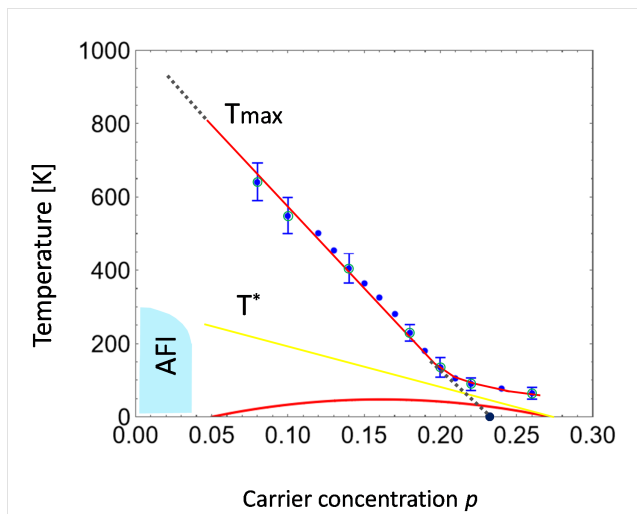


FIGURE 4. (Color online) The magnetic characteristic temperature T_{max} determined from the spin susceptibility of $\text{La}_{2-x}\text{Sr}_x\text{CuO}_4$ measured by Nakano et al.[46]. Points for T_{max} with error bars are deduced from the fits of Fig. 2a; the remaining points are inferred from an interpolation procedure of the data. One can see that the extrapolation of the straight line at $T = 0$ is 0.23.

$\chi(T)$ is given by Eq. 2 with an additional constant arising from the electronic Pauli susceptibility :

$$\chi(T) = \chi_{Pauli} + \chi_{AF}(T) \quad (3)$$

From the fits of the data, we extract the doping dependence of T_{max} which accurately reproduces the results of Nakano et al [46] : $T_{max}(p)$ follows a straight line for a wide doping range, in agreement with early calculations [52], which extrapolates to zero at a value $p \approx 0.23$ at $T = 0$. However, $T_{max}(p)$ does not vanish but saturates in the overdoped regime, suggesting that the magnetism is persistent there.

The case of LSCO, where both T_c and T^* are a factor of two smaller than in BSCCO and YBCO, allows to explain very satisfactorily the series of observations in terms of the AF magnetic contribution. We now focus our attention on the other cuprates, where a more complete analysis is needed.

General analysis of the susceptibility

In order to describe the susceptibility of cuprates in a more general way, we need to extend the model described above. In particular, one has to include the effect of the pseudogap in the electronic DOS.

For this purpose, we write the susceptibility as a sum of the following contributions :

$$\chi(T) = \chi_0 + \chi_{AF}(T) + \chi_{Pauli}(T) + \chi_{dia}(T) \quad (4)$$

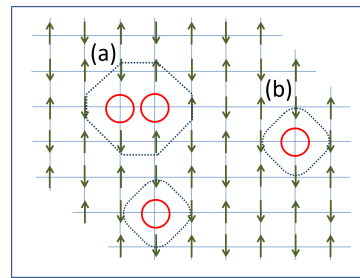


FIGURE 5. (Color online) Schematic diagram of a pairon (a) versus a hole (b) in their local antiferromagnetic environment, on the scale of the antiferromagnetic correlation length, ξ_{AF} .

The first term is a constant, independent of temperature and doping, which groups together the atomic core and Van Vleck contributions to the susceptibility. The second term, $\chi_{AF}(T)$, is the response of the AF square lattice, as mentioned previously. The third term, $\chi_{Pauli}(T)$, is the electronic term arising from the delocalized electrons at the Fermi level. The last term, $\chi_{dia}(T)$, is the diamagnetic contribution arising from superconducting currents, relevant close to T_c .

We now focus on the electronic term that we will evaluate in the framework of the pairon model [53]. In a previous work, we have proposed that in cuprate superconductors pairing occurs in an unconventional way, very distinct from the BCS scenario where Cooper pairs are bound via phonon exchange. In high- T_c cuprates, hole pairs (which we call ‘pairons’) form directly as a result of their local antiferromagnetic environment [33, 34], without phonon or magnon exchange (see Fig.5). This binding mechanism provides an energy gain of the order of J , the AF exchange energy, as confirmed by early numerical calculations [54–58]. The characteristic temperature of pairon formation is by definition T^* , directly proportional to J [33, 36].

Pairons are composite bosons which condense in the collective superconducting state below T_c , as a result of pairon-pairon interactions, which sets the global phase coherence. In this approach, two energy scales are thus relevant, the gap Δ_p (pairon binding energy in the SC state) and β_c , the condensation energy per pair [53]. The first is associated with the pseudogap temperature T^* , while the second is proportional to T_c ($\beta_c \simeq 2.2k_B T_c$). Thus, contrary to the BCS theory, here the gap is not the order parameter since it does not vanish at T_c .

Both ARPES [27, 28, 59] and tunneling [15, 60, 61] measurements have confirmed that the antinodal gap is still present at the critical temperature and closes at a higher temperature T^* . Furthermore, Fig. 6 illustrates two astonishing aspects : first the measured temperature of the closing of the gap, T^* , is directly proportional to the zero temperature gap, with a proportionality factor given by the relation $\Delta_p \approx 2.2k_B T^*$. The factor 2.2 has been previously determined from detailed fits of ARPES and

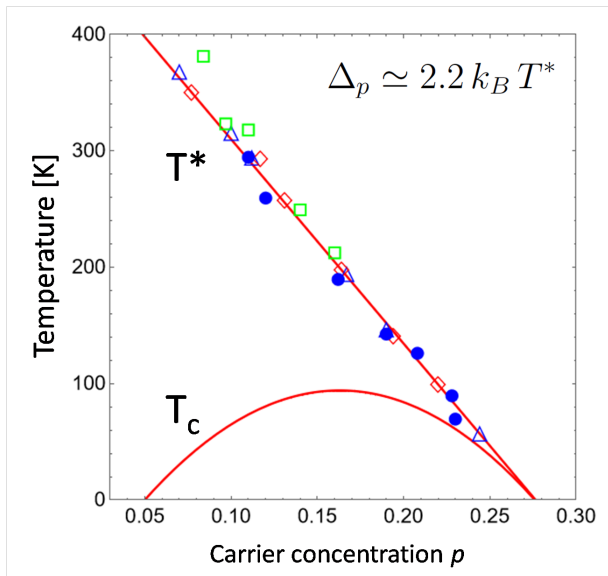


FIGURE 6. (Color online) open triangles and squares : anti-nodal energy gap measured at $T = 0$ expressed in Kelvin, $\Delta_p/2.2k_B$. Filled circles : direct temperature measurement of the gap closing at the higher value T^* . The data points are ARPES measurements in BSCCO taken from the article of Vishik et al. [27] and Hashimoto et al. [59].

tunneling spectra [33, 36]. Secondly, the dependence of the gap Δ_p is practically linear with carrier concentration.

Given that the Pauli contribution to the susceptibility is proportional to the DOS at the Fermi energy, in what follows we calculate this quantity. In a BCS superconductor, above the critical temperature the Pauli susceptibility should be roughly independent of temperature. On the contrary, in the pairon model for cuprates, involving pair excitations and pair dissociations, the DOS at the Fermi energy depends explicitly on temperature up to $\sim T^*$.

More precisely, at finite temperature, pairons are excited out of the condensate following Bose-Einstein statistics and dissociate into quasiparticles, preferentially close to the node, leading to Fermi arcs [62]. This effect, as studied in Ref. [36] gives rise to a temperature-dependent DOS :

$$N_{ex}(E, T) = \sum_i n_i(\varepsilon_i, T) \int \frac{d\theta}{2\pi} N^i(E, \Delta_i(\theta)) \quad (5)$$

where $N^i(E, \Delta_i(\theta))$ is the standard angular-dependent quasiparticle DOS, ε_i are the excited pairon energies, $n_i(\varepsilon_i, T)$ is the number of excited pairons with associated quasiparticles $E_k^i = \sqrt{\varepsilon_k^2 + \Delta_i^2}$.

Given the density of pair states $P_0(\varepsilon_i)$, one has :

$$n_i(\varepsilon_i, T) = AP_0(\varepsilon_i)f_{BE}(\varepsilon_i) \quad (6)$$

where $f_{BE}(\varepsilon) = 1/\left(\exp\left(\frac{\varepsilon - \mu_b}{k_B T}\right) - 1\right)$ is the Bose-

Einstein distribution and where A is a normalization factor. We further impose particle conservation $\sum_i n_i(\varepsilon_i, T) = n_0$, where n_0 is the number of pairs, which determines both the constant A and the chemical potential $\mu(T)$ given that $\mu_b(T) = 0$ for $T \leq T_c$.

As in our previous work, the density of pairon excited states is assumed to have a Lorentzian form :

$$P_0(\varepsilon_i) = \frac{\sigma_0^2}{[(\varepsilon_i - \beta_c)^2 + \sigma_0^2]} \quad (7)$$

where σ_0 is the width of the distribution. The evaluation of Eq. 5 needs the relation between the boson excitations (ε_i) and the associated quasiparticles (E_k^i). We use the relation : $\varepsilon_i = \Delta_i - \Delta_p(T, \theta)$, where $\Delta_p(T, \theta)$ is the standard d -wave gap with a smooth and decreasing temperature dependence as in Ref. [63]. With these considerations, we can write :

$$N_{ex}(E, T) = N_n \sum_i n_i(\varepsilon_i, T) \int \frac{d\theta}{2\pi} \frac{E}{\sqrt{E^2 - (\varepsilon_i + \Delta_p(T, \theta))^2}} \quad (8)$$

where N_n is the normal DOS.

Equation 8 leads to a T-dependent DOS at the Fermi energy $N_{ex}(0, T)$ which varies significantly up to the pseudogap temperature T^* . The associated Pauli susceptibility is then determined by the standard formula :

$$\chi_{Pauli}(T) \propto \int -\frac{\partial f(E, T)}{\partial E} N_{ex}(E, T) dE \quad (9)$$

where $f(E, T)$ is the Fermi-Dirac distribution. The precise numerical calculation is plotted for different doping values in Fig. 3 (see supplementary materials for further details on the calculation of the DOS).

Finally, close to the SC transition (for $T \lesssim T_c + \Delta T$), the aforementioned diamagnetic current term must be included. We use the very simple form :

$$\chi_{dia}(T) = A_{dia} \exp\left(-\frac{T - T_c}{\Delta T}\right) \quad (10)$$

where A_{dia} is a negative constant and ΔT characterizes the existence of diamagnetic currents above T_c .

Fits of the data

We have fitted the experimental susceptibility for the four materials (LSCO, Y-BSCCO, BSCCO, YBCO). Results are shown in Fig. 7. Let us point out that the same function was used with success for the four different compounds, apart from a small supplementary ‘Curie’ paramagnetic term ($\propto 1/T$) term in the fit for LSCO in the overdoped regime [64].

The fit procedure contains the four terms of equation 4, but the overall shape is clearly dominated by the magnetic plus the Pauli terms. The constant χ_0 is fixed for each

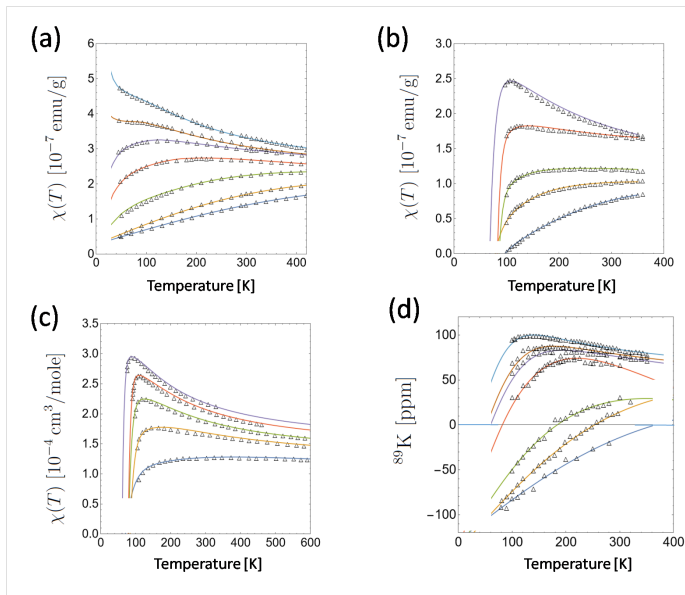


FIGURE 7. (Color online) Colored full lines are the fits, using the analysis described in the text, to the experimental data of Fig. 2 (dots), reported for a) $\text{La}_{1-x}\text{Sr}_x\text{CuO}_4$ by Nakano et al. [46], b) $\text{Bi}_2\text{Sr}_2\text{Ca}_{1-x}\text{Y}_x\text{Cu}_2\text{O}_8$ by Oda et al. [47], c) $\text{Bi}_2\text{Sr}_2\text{CaCu}_2\text{O}_{8+y}$ by Allgeier et al. [48]. d) Knight shift measured in $\text{YBa}_2\text{Cu}_3\text{O}_{6+y}$ [49].

material for the lowest doping value (within a variation of 10 percent for Y-BSCCO).

We extract from the fits the values of the parameters, T_{max} , T^* and the Pauli amplitude, as a function of doping. Results are plotted in Fig. 8 for LSCO (left panel), YBCO (middle panel), for oxygen and Y-doped BSCCO (right panel). A striking feature is that, for all materials, $T_{max}(p)$ decreases linearly as a function of doping up to slightly overdoped regime ($p \simeq 0.19$). This straight T_{max} line extrapolates at $T = 0$ to a doping value $p \simeq 0.23$ for LSCO and YBCO and $p \simeq 0.20$ for BSCCO. Towards the top of the dome, $T_{max}(p)$ has a more complex behavior deviating from linearity and saturating in the overdoped regime. These findings extend the work of Nakano et al. on LSCO [46].

The pseudogap temperature T^* deduced from the fits (see Fig. 8, green dashed line) follows a straight line for LSCO, YBCO and BSCCO, as a function of doping, throughout the SC dome. For Y-doped BSCCO, small deviations from linearity arises near the top of the dome. In addition, for all the four compounds studied, T^* is higher than T_c for all doping values and thus never crosses the T_c -dome. In conclusion, the $T^*(p)$ line extracted from the susceptibility curves closely matches the values obtained by ARPES [27].

The Pauli amplitude deduced from the fits is plotted in Fig. 9. It is increasing as a function of p for BSCCO and LSCO and YBCO. For Y-doped BSCCO, it is first monotonically increasing, but then decreases abruptly in

the highly overdoped regime. In spite of the relative uncertainty, our results for the amplitude are similar to the behavior of $\gamma_N(p)$, the gamma coefficient of the specific heat in the normal state [65, 66]. Indeed, for a standard metal, both γ_N and χ_{Pauli} are proportional to the DOS at the Fermi energy.

Discussion

Two temperature scales emerge from our analysis, T^* the temperature at which the pseudogap in the electronic DOS at the Fermi level opens, and T_{max} the characteristic temperature of antiferromagnetic correlations. The $T^*(p)$ line is found to be tangential to the superconducting dome, and therefore never crosses the T_c line. The magnetic scale T_{max} behaves in a different way : in the four materials we have considered, it decreases linearly as a function of p , with a steeper slope, up to the slightly overdoped value $p \sim 0.19$. It then saturates in the overdoped region, in agreement with the persistence of magnetic correlations seen up to p_c reported by [45, 67, 68] and even beyond [69]. In addition, the extrapolation of the linear behavior gives a critical value close to $p = 0.2$ in the four materials.

Although very prominent, this magnetic temperature scale has been improperly attributed to the pseudogap temperature. For example, the ‘pseudogap’ temperature inferred from Hall measurement for LSCO is very close to our $T_{max}(p)$. The confusion between T^* and T_{max} explains the contradiction between the phase diagrams deduced from susceptibility, transport measurements, on the one hand, and those deduced from spectroscopic measurements on the other hand.

Transport and susceptibility measurements are not direct probes of the DOS at the Fermi energy since they are not only sensitive to mobile carriers at the Fermi level, but also to their multiple diffusion processes. On the contrary, tunneling spectroscopy and ARPES directly probe the quasiparticle peaks with a high precision. This might explain the apparent contradiction between the two different pseudogap lines found in the literature.

The interpretation of this new phase diagram within the pairon model is at this point speculative, because of the absence of exact solutions for microscopic models. Indeed, it is important to note that another model with a similar temperature-dependent DOS at the Fermi energy, i.e. decreasing below a characteristic temperature T^* , would have given qualitatively the same behavior for $T^*(p)$. Therefore, one cannot exclude other interpretations for the origin of the pseudogap. A pseudogap line tangential SC dome is also found by Marino et al. [70–72], with a model where the pseudogap is attributed to the condensation of excitons.

In this work, we interpret the pseudogap as being due to the formation of incoherent hole pairs or pairons. In

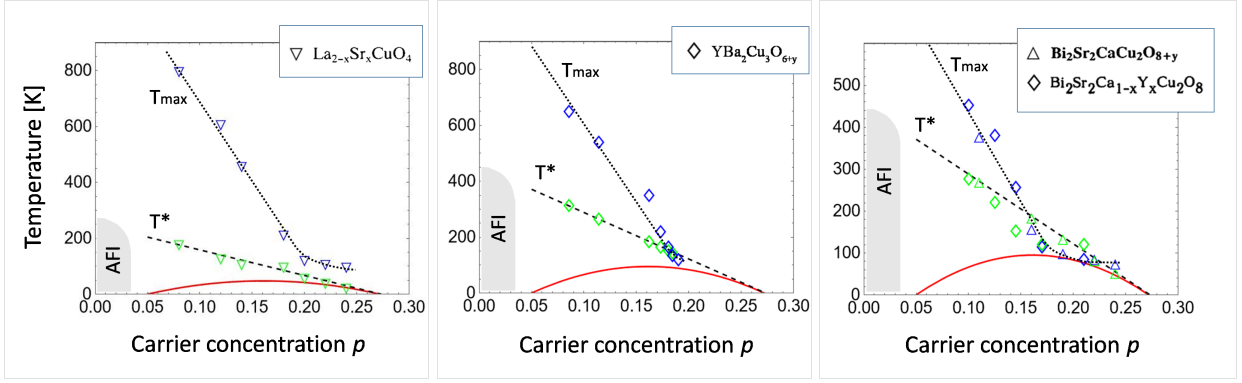


FIGURE 8. (Color online) T^* and T_{max} as a function doping, as deduced from the fits for the four materials of Fig. 7. Note that both $T_{max}(p)$ and $T^*(p)$, for a wide range of p , display very similar laws. $T^*(p)$ runs tangential to the dome and seems to approach, at low doping, the Néel temperature of the AF insulator state (shaded area), as also noted in [73]. $T_{max}(p)$ remarkably follows a universal law for the four materials.

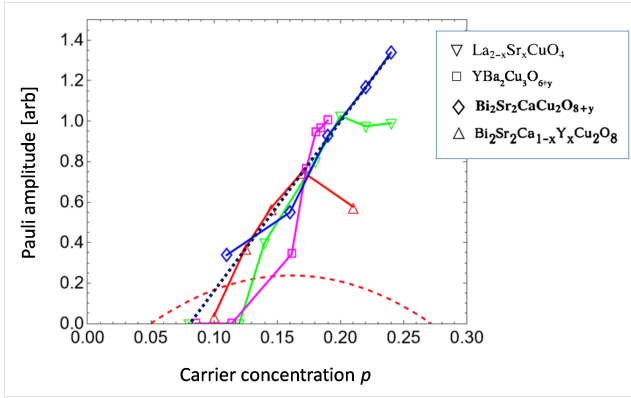


FIGURE 9. (Color online) Pauli (pairon) amplitude as deduced from the fits as a function of the carrier concentration. (Dotted line : T_c dome for convenience). The Pauli contribution to the susceptibility is obtained by calculating the temperature-dependent DOS at the Fermi energy within an energy window of the order $k_B T$ (see Eq. 9).

this scenario, there is a natural link between T_{max} and T^* . Although having a very different doping behavior, it is important to stress that both temperature scales, T_{max} and T^* , are proportional to the same energy scale, the exchange energy J . For the undoped 2D square lattice T_{max} is given by [51] :

$$k_B T_{max} \approx 1.12 J \times S(S+1) \quad (11)$$

whereas for T^* , a mean-field equation for pairons allows to write [33] :

$$2.2 k_B T^* \approx J \left(1 - \frac{p}{p_c}\right) \quad (12)$$

where $p_c=0.27$ is the doping for which superconductivity vanishes at the dome extremity (see Fig. 1, left panel). Note that for LSCO, the T^* and T_c are lower by a factor of two. The factor 2.2 in Eq. 12 should then be replaced

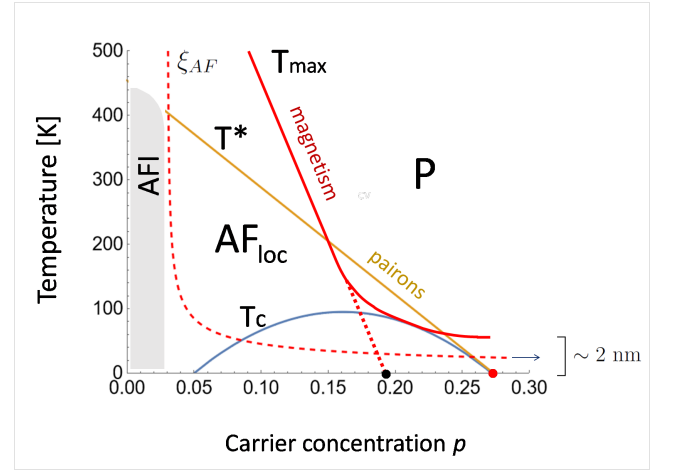


FIGURE 10. (Color online) Phase diagram for BSCCO deduced from the susceptibility data : T_{max} (red line), T^* (yellow line) as a function of p , the hole concentration. The critical temperature for BSCCO (blue line) and the antiferromagnetic correlation length (dashed line) are also indicated. ξ_{AF} is approximated by the average distance between holes, as found by Birgeneau et al. [74]. The $T_{max}(p)$ line separates the phase diagram into two regions : on the left ($T < T_{max}(p)$) characterized by local AF order (AF_{loc}) and on the right ($T > T_{max}(p)$), characterized by strong magnetic fluctuations (P).

by 1.1. The validity of Eq. 12 for $T^*(p)$, as determined by electron spectroscopies, is illustrated Fig. 6. It is quantitatively compatible with the PG temperature deduced from the susceptibility data.

In addition, for the magnetic scale, we find the surprisingly simple relation

$$T_{max}(p) \approx 960 K (1 - 5p) \quad (13)$$

which extrapolates to zero at $p=0.2$. These two simple linear laws for T_{max} and T^* give a slope difference of about a factor of two, except for LSCO, and a crossing

point near the top of the dome. The above linear law for $T_{max}(p)$ is close to the energy gap E_g/k_B deduced from both specific heat [31] and susceptibility [29, 30].

A summary of our findings is presented in the phase diagram in Fig. 10. The $T_{max}(p)$ line clearly separates the cuprate phase diagram in two main regions, to the left and to the right of the crossing point of $T_{max}(p)$ and $T^*(p)$. For $p \lesssim 0.16$, the pseudogap temperature T^* is smaller, or even much smaller, than T_{max} . This means that pairon formation occurs in the region of local AF order (indicated by AF_{loc} in Fig. 10). Therefore, above T_c pairons dissociate in a system with strong magnetic correlations.

On the other hand, to the right of the crossing point for $p > 0.16$, T_{max} and T^* are close and pairons dissociate in a different magnetic environment (indicated by ‘P’ in Fig. 10). Since we know from the fits that the susceptibility is close to a Curie law, we identify this region as ‘paramagnetic’. In this region, the spin-spin correlations are small ($T_{max} \sim 50 - 60\text{K}$) and the correlation length ξ_{AF} is of the order of a few lattice constants [74].

We see that crossing the top of the dome, from left to right, there is a clear change of regime which should affect all physical quantities. First, the magnetic response changes from strong antiferromagnetic correlation (AF local) to weak correlations (P). Second, pairon decay into quasiparticles becomes much more dominant, leading to the increasing Fermi-arcs, as reported in the literature [62] and confirmed by the Pauli amplitude in Fig. 9. Consequently, quasiparticles above T_c must have a significantly different self-energy and spectral function, as possibly seen in [75]. This should affect the resistivity, specific heat and Knight shift.

Finally, as indicated in Fig. 10, in the overdoped regime both T^* and T_c approach each other and finally vanish at $p_c = 0.27$, the critical point at the end of the superconducting dome. On the other hand, magnetic correlations persist in the overdoped regime [69, 76, 77] and the magnetic scale T_{max} remains finite.

Conclusion

In this paper, we have tackled the issue of two contradictory phase diagrams emerging from transport, specific heat, susceptibility on the one hand versus electron spectroscopies on the other hand.

To this end, we analyzed the magnetic susceptibility, $\chi(T)$, measured in high- T_c cuprates in $\text{La}_{1-x}\text{Sr}_x\text{CuO}_4$, $\text{Bi}_2\text{Sr}_2\text{Ca}_{1-x}\text{Y}_x\text{Cu}_2\text{O}_8$, $\text{Bi}_2\text{Sr}_2\text{CaCu}_2\text{O}_{8+y}$ as well as the Knight shift measured in $\text{YBa}_2\text{Cu}_3\text{O}_{6+y}$. Our analysis of $\chi(T)$ contains two major contributions, the magnetic response of the 2D AF lattice, and the Pauli term containing the Fermi level density of states. It is remarkable that the same function matches the measured $\chi(T)$ for all four materials from underdoped to overdoped regimes.

To summarize the results :

- i) Two temperature scales emerge from the analysis : T_{max} , the characteristic scale for antiferromagnetic correlations, and T^* , characterizing the opening of the pseudogap in the electronic density of states at the Fermi level. The DOS was calculated in the framework of the pairon model, wherein hole pairs form due to their local antiferromagnetic environment below T^* . The measured Pauli term in $\chi(T)$ is therefore fully consistent with excited pairons existing above T_c .
- ii) The magnetic contribution describes very well the overall shape of the susceptibility. In particular, $T_{max}(p)$ decreases linearly over a wide range of hole doping p but saturates in the overdoped regime. The extrapolated line ends at a critical doping $p \sim 0.2$ for all the materials studied. Concomitantly, $T^*(p)$ is linear, with a smaller slope, and tangential to the superconducting dome, as confirmed by electron spectroscopies.
- iii) In our concluding phase diagram, we identify two different regions, relative to the crossing point of T_{max} and T^* . It implies a significant change of behavior in the magnetic correlations occurring from left to right at the top of the superconducting dome. Correspondingly, from underdoped to overdoped, we expect a qualitative change in the pairon dissociation, implying modifications in the quasiparticle spectral function.
- iv) Our findings strongly suggest that the characteristic temperature $T_{max}(p)$ inferred from susceptibility and transport measurements has been incorrectly interpreted as the pseudogap temperature. Furthermore, the linear behavior found for $T^*(p)$, indicates that the same physics governs the pseudogap formation all along the superconducting dome.
- v) We interpret the pseudogap as being due to the formation of incoherent hole pairs, or pairons. Remarkably, in this scenario, the two temperature scales $T_{max}(p)$ and $T^*(p)$ coexist in the same phase diagram and are proportional to the same energy, the exchange energy J .

Supplementary material, on the model and data analysis, is available upon request from the corresponding author⁽¹⁾.

Acknowledgments

[1] J. G. Bednorz, K. A. Müller, Possible high T_c superconductivity in the Ba–La–Cu–O system, *Zeitschrift für Physik B Condensed Matter* **64**, 189 (1986).

- [2] T. Timusk and B. Statt, The pseudogap in high-temperature superconductors : An experimental survey. *Rep. Prog. Phys.* **62**, 61-122 (1999).
- [3] W. W. Warren, Jr., R. E. Walstedt, G. F. Brennert, R. J. Cava, R. Tycko, R. F. Bell, and G. Dabbagh, Cu spin dynamics and superconducting precursor effects in planes above T_c in $\text{YBa}_2\text{Cu}_3\text{O}_{6.7}$, *Phys. Rev. Lett.* **62**, 1193 (1989).
- [4] H. Alloul, T. Ohno, and P. Mendels, ^{89}Y NMR evidence for a fermi-liquid behavior in $\text{YBa}_2\text{Cu}_3\text{O}_{6+x}$, *Phys. Rev. Lett.* **63**, 1700 (1989).
- [5] L. D. Rotter, Z. Schlesinger, R. T. Collins, F. Holtzberg, C. Field, U. W. Welp, G. W. Crabtree, J. Z. Liu, Y. Fang, K. G. Vandervoort, and S. Fleshler, Dependence of the infrared properties of single-domain $\text{Ba}_2\text{Cu}_3\text{O}_{7-y}$ on oxygen content, *Phys. Rev. Lett.* **67**, 2741 (1991).
- [6] C. C. Homes, T. Timusk, R. Liang, D. A. Bonn, and W. N. Hardy, Optical conductivity of c axis oriented $\text{YBa}_2\text{Cu}_3\text{O}_{6.70}$: Evidence for a pseudogap, *Phys. Rev. Lett.* **71**, 1645 (1993).
- [7] G. Shirane, R. J. Birgeneau, Y. Endoh, P. Gehring, M. A. Kastner, K. Kitazawa, H. Kojima, I. Tanaka, T. R. Thurston, and K. Yamada, Temperature dependence of the magnetic excitations in $\text{La}_{1.85}\text{Sr}_{0.15}\text{CuO}_4$ ($T_c = 33\text{K}$), *Phys. Rev. Lett.* **63**, 330 (1989).
- [8] J. Rossat-Mignod, L.P. Regnault, C. Vettier, P. Burlet, J.Y. Henry and G. Lapertot, Investigation of the spin dynamics in $\text{YBa}_2\text{Cu}_3\text{O}_{6+x}$ by inelastic neutron scattering, *Physica B* **169**, 58-65 (1991).
- [9] T. Ito, K. Takenaka, and S. Uchida, Systematic deviation from T-linear behavior in the in-plane resistivity of $\text{YBa}_2\text{Cu}_3\text{O}_{7-y}$: Evidence for dominant spin scattering, *Phys. Rev. Lett.* **70**, 3995 (1993).
- [10] B. Bucher, P. Steiner, J. Karpinski, E. Kaldis, and P. Wachter, Influence of the spin gap on the normal state transport in $\text{YBa}_2\text{Cu}_4\text{O}_8$, *Phys. Rev. Lett.* **70**, (1993).
- [11] B. Batlogg, H. Y. Hwang, H. Takagi, R. J. Cava, H. L. Kao and J. Kwo, Normal State Phase Diagram of $(\text{La,Sr})_2\text{CuO}_4$ from Charge and Spin Dynamics, *Physica C* **235-240**, 130 (1994).
- [12] T. Watanabe, T. Fujii, A. Matsuda ,Anisotropic transport properties of impurity (Co) doped and oxygen controlled single-crystal $\text{Bi}_2\text{Sr}_2\text{CaCu}_2\text{O}_{8+\delta}$: Evidence of temperature-dependent interlayer coupling and a pseudogap, *Physica C* **282-287**, 1169 (1997).
- [13] J. W. Loram, K. A. Mirza, J. M. Wade, J. R. Cooper, W. Y. Liang, The electronic specific heat of cuprate superconductors, *Physica C* **235-240**, Pages 134 (1994).
- [14] H. J. Tao, Farun Lu, and E. L. Wolf, Observation of pseudogap in $\text{Bi}_2\text{Sr}_2\text{CaCu}_2\text{O}_{8+\delta}$ single crystals with electron tunneling spectroscopy, *Physica C* **282-287**, 1507 (1997).
- [15] Ch. Renner, B. Revaz, J.-Y. Genoud, K. Kadowaki, and Ø. Fischer, Pseudogap precursor of the superconducting gap in under- and overdoped $\text{Bi}_2\text{Sr}_2\text{CaCu}_2\text{O}_{8+\delta}$, *Phys. Rev. Lett.*, **80** 149 (1998).
- [16] H. Ding, T. Yokoya, J. C. Campuzano, T. Takahashi, M. Randeria, M. R. Norman, T. Mochiku, K. Kadowaki and J. Giapintzakis, Spectroscopic evidence for a pseudogap in the normal state of underdoped high- T_c superconductors, *Nature* **382**, 51 (1996).
- [17] A. G. Loeser, D. S. Dessau , Z.-X. Shen, Doping dependence of Doping dependence of $\text{Bi}_2\text{Sr}_2\text{CaCu}_2\text{O}_{8+\delta}$ in the normal state, *Physica C* **263**, 208 (1996).
- [18] J. Bardeen, L. Cooper, J. Schrieffer, Theory of Superconductivity, *Phys. Rev.* **108** 1175 (1957).
- [19] A. A. Kordyuk, Pseudogap from ARPES experiment : Three gaps in cuprates and topological superconductivity, *Low Temp. Phys.* **41**, 319 (2015).
- [20] Ø. Fischer, M. Kugler, I. Maggio-Aprile, C. Berthod and C. Renner, Scanning tunneling spectroscopy of the cuprates, *Rev. Mod. Phys.* **79**, 353 (2007).
- [21] A. Damascelli, Z. Hussain, and Z.-X. Shen, Angle-resolved photoemission studies of the cuprate superconductors, *Rev. Mod. Phys.* **75**, 473 (2003).
- [22] S. Hufner, M. A. Hossain, A Damascelli, and G. A. Sawatzky, Two gaps make a high-temperature superconductor?, *Rep. Prog. Phys.*, **71**, 062501 (2008).
- [23] Z. Konstantinović, Z.Z. Li, H. Raffy, Evolution of the resistivity of single-layer $\text{Bi}_2\text{Sr}_{1.6}\text{La}_{0.4}\text{CuO}_y$ thin films with doping and phase diagram, *Physica C : Superconductivity* **351**, Pages 163 (2001).
- [24] S. H. Naqib, J. R. Cooper, J. L. Tallon, C. Panagopoulos, Temperature dependence of electrical resistivity of high- T_c cuprates—from pseudogap to overdoped regions, *Physica C* **387**, 365 (2003).
- [25] E. Sterpetti, J. Biscaras, A. Erb and A. Shukla, Comprehensive phase diagram of two-dimensional space charge doped $\text{Bi}_2\text{Sr}_2\text{CaCu}_2\text{O}_{8+x}$, *Nat. Commun.* **8**, 2060 (2017).
- [26] C. Proust and L. Taillefer, Annual Review of Condensed Matter Physics **10**, 409 (2019).
- [27] I. M. Vishik, M. Hashimoto, R.-H. He, W.-S. Lee, F. Schmitt, D. Lu, R. G. Moore, C. Zhang, W. Meevasana, T. Sasagawa, S. Uchida, Kazuhiro Fujita, S. Ishida, M. Ishikado, Y. Yoshida, H. Eisaki, Z. Hussain, T. P. Devereaux, and Z.-X. Shen, Phase competition in trisected superconducting dome, *PNAS* **109**, 18332 (2012).
- [28] M. Hashimoto, T. Yoshida, K. Tanaka, A. Fujimori, M. Okusawa, S. Wakimoto, K. Yamada, T. Kakeshita, H. Eisaki, and S. Uchida, Distinct doping dependences of the pseudogap and superconducting gap of $\text{La}_{2-x}\text{Sr}_x\text{CuO}_4$ cuprate superconductors, *Phys. Rev. B* **75**, 140503(R) (2007).
- [29] S. H. Naqib, J. R. Cooper, Effect of the pseudogap on the uniform magnetic susceptibility of $\text{Y}_{1-x}\text{Ca}_x\text{Ba}_2\text{Cu}_3\text{O}_{7+\delta}$, *Physica C : Superconductivity* **460-462**, 750-752 (2007).
- [30] S. H. Naqib and R. S. Islam, Extraction of the pseudogap energy scale from the static magnetic susceptibility of single and double CuO_2 plane high- T_c cuprates, *Supercond. Sci. Technol.* **21**, 105017 (2008).
- [31] J. W. Loram, K. A. Mirza, J. R. Cooper, J. L. Tallon, Specific heat evidence on the normal state pseudogap, *Journal of Physics and Chemistry of Solids* **59**, 2091(1998).
- [32] J. W. Loram, J. Luo, J. R. Cooper, W. Y. Liang, J. L. Tallon, Evidence on the pseudogap and condensate from the electronic specific heat, *Journal of Physics and Chemistry of Solids* **62**, 59 (2001).
- [33] W. Sacks, A. Mauger and Y. Noat, Cooper pairs without glue in high- T_c superconductors : A universal phase diagram, *Euro. Phys. Lett* **119**, 17001 (2017).
- [34] Y. Noat, A. Mauger and W. Sacks, Single origin of the nodal and antinodal gaps in cuprates, *Euro. Phys. Lett* **126**, 67001 (2019).
- [35] W. Sacks, A. Mauger and Y. Noat, Unconventional temperature dependence of the cuprate excitation spectrum, *Eur. Phys. J. B* **89**, 183 (2016).
- [36] W. Sacks, A. Mauger and Y. Noat, Origin of the Fermi arcs in cuprates : a dual role of quasiparticle and pair

- excitations, *Journal of Physics : Condensed Matter*, **30**, 475703 (2018).
- [37] L. F. Lopes, J. Paola Peña, Jacob Schaf, Milton A. Tumeleiro, Valdemar N. Vieira, Paulo Pureur, Magnetic susceptibility in the normal phase of $\text{Bi}_2\text{Sr}_2\text{CaCu}_2\text{O}_{8+\delta}$ single crystals, *Physica B : Condensed Matter* **536**, 855 (2018).
- [38] T. Nakano, N. Momono, M. Oda, and M. Ido, Correlation between the Doping Dependences of Superconducting Gap Magnitude $2\Delta_0$ and Pseudogap Temperature T^* in High- T_c Cuprates, *J. Phys. Soc. Jpn.* **67**, 2622 (1998).
- [39] David C. Johnston, Magnetic Susceptibility Scaling in $\text{La}_{2-x}\text{Sr}_x\text{CuO}_{4-y}$, *Phys. Rev. Lett.* **62**, 957 (1989).
- [40] J. B. Torrance, A. Bezing, A. I. Nazzal, T. C. Huang, S. S. P. Parkin, D. T. Keane, S. J. LaPlaca, P. M. Horn, and G. A. Held, Properties that change as superconductivity disappears at high-doping concentrations in $\text{La}_{2-x}\text{Sr}_x\text{CuO}_4$, *Phys. Rev. B* **40**, 8872 (1989).
- [41] T. Takagi, T. Ido, S. Ishibashi, M. Uota, S. Uchida, and Y. Tokura, Superconductor-to-nonsuperconductor transition in $(\text{La}_{1-x}\text{Sr}_x)_2\text{CuO}_4$ as investigated by transport and magnetic measurements, *Phys. Rev. B* **40**, 2254 (1989).
- [42] R. Yoshizaki, N. Ishikawa, H. Sawada, E. Kita, A. Tasaki, Magnetic susceptibility of normal state and superconductivity of $\text{La}_{2-x}\text{Sr}_x\text{CuO}_4$, *Physica C* **166**, 417 (1990).
- [43] M. Oda, T. Ohguro, H. Matsuki, N. Yamada, and M. Ido, Magnetism and superconductivity in doped La_2CuO_4 , *Phys. Rev. B* **41**, 2605(R) (1990).
- [44] M. Oda, K. Hoya, R. Kubota, C. Manabe, N. Momono, T. Nakano, M. Ido, Strong pairing interactions in the underdoped region of $\text{Bi}_2\text{Sr}_2\text{CaCu}_2\text{O}_{8+\delta}$, *Physica C* **281**, 135 (1997).
- [45] S. Wakimoto, R. J. Birgeneau, A. Kagedan, Hyun-kyung Kim, I. Swainson, K. Yamada, and H. Zhang, Magnetic properties of the overdoped superconductor $\text{La}_{2-x}\text{Sr}_x\text{CuO}_4$ with and without Zn impurities, *Phys. Rev. B* **72**, 064521 (2005).
- [46] T. Nakano, M. Oda, C. Manabe, N. Momono, Y. Miura, and M. Ido, Magnetic properties and electronic conduction of superconducting $\text{La}_{2-x}\text{Sr}_x\text{CuO}_4$, *Phys. Rev. B* **49**, 16000 (1994).
- [47] M. Oda, H. Matsuki, M. Ido, Common features of magnetic and superconducting properties in Y-doped $\text{Bi}_2(\text{Sr},\text{Ca})_3\text{Cu}_2\text{O}_8$ and Ba(Sr)-doped La_2CuO_4 , *Solid State Communications* **74**, 1321 (1990).
- [48] C. Allgeier and J. S. Schilling, Magnetic susceptibility in the normal state : A tool to optimize T_c within a given superconducting oxide system, *Phys. Rev. B* **48**, 9747 (1993).
- [49] Henry Alloul, NMR in Correlated Electron Systems : Illustration on the Cuprates, in E. Pavarini, E. Koch, J. van den Brink, and G. Sawatzky (eds.), *Quantum Materials : Experiments and Theory Modeling and Simulation*, **6**, 13.1 (2016).
- [50] J. L. Tallon and J. W. Loram, Field Dependent specific heat of the canonical underdoped cuprate superconductor $\text{YBa}_2\text{Cu}_4\text{O}_8$, *Scientific Reports* **10**, 22288 (2020).
- [51] M. E. Lines, The quadratic-layer antiferromagnet, *J. Phys. Chem. Solids* . **31**, 101 (1970).
- [52] R. L. Glenister, and R. R. P. Sing, Temperature and doping dependence of the magnetic susceptibility in the cuprates, *Journal of Applied Physics* **73**, 6329 (1993).
- [53] W. Sacks, A. Mauger, Y. Noat, Pair-pair interactions as a mechanism for high- T_c superconductivity, *Superconduct. Sci. Technol.*, **28** 105014 (2015).
- [54] Efthimios Kaxiras and Efstratios Manoussakis, Hole dynamics in the two-dimensional strong-coupling Hubbard Hamiltonian, *Phys. Rev. B* **38**, 866(R) (1988).
- [55] J. Bonča, P. Prelovšek, and I. Sega, Exact-diagonalization study of the effective model for holes in the planar antiferromagnet, *Phys. Rev. B* **39**, 7074 (1989).
- [56] J. A. Riera and A. P. Young, Binding of holes in one-band models of oxide superconductors, *Phys. Rev. B* **39**, 9697(R) (1989).
- [57] Y. Hasegawa and D. Poilblanc, Hole dynamics in the t-J model : An exact diagonalization study, *Phys. Rev. B* **40**, 9035 (1989).
- [58] Didier Poilblanc, José Riera and Elbio Dagotto, d-wave bound state of holes in an antiferromagnet, *Phys. Rev. B* **49**, 12318 (1994).
- [59] M. Hashimoto, I.M. Vishik, R.-H. He, T.P. Devereaux and Z.-X. Shen, Energy gaps in high-transition-temperature cuprate superconductors, *Nature Physics* **10**, 483 (2014).
- [60] K. K. Gomes, A.N. Pasupathy, A. Pushp, C. Parker, S. Ono, Y. Ando, G. Gu, A. Yazdani, Mapping of the formation of the pairing gap in $\text{Bi}_2\text{Sr}_2\text{Ca}_2\text{CuO}_{8+\delta}$, *Journal of Physics and Chemistry of Solids* **69**, 3034 (2008).
- [61] R. Sekine, S. J. Denholme, A. Tsukada, S. Kawashima, M. Minematsu, T. Inose, S. Mikusu, K. Tokiwa, T. Watanabe, and N. Miyakawa, Characteristic features of the mode energy estimated from tunneling conductance on $\text{TlBa}_2\text{Ca}_2\text{Cu}_3\text{O}_{8.5+\delta}$, *J. Phys. Soc. Jpn.* **85**, 024702 (2016).
- [62] M. R. Norman, H. Ding, M. Randeria, J.C. Campuzano, T. Yokoya, T. Takeuchi, T. Takahashi, T. Mochiku, K. Kadowaki, P. Guptasarma and D. G. Hinks, Destruction of the Fermi surface in underdoped high- T_c superconductors, *Nature* **392**, 157160 (1998).
- [63] Y. Noat, A. Mauger, M. Nohara, H. Eisaki, W. Sacks , How ‘pairons’ are revealed in the electronic specific heat of cuprates, *Solid State Communications* **323**, 114109 (2021).
- [64] T. Nakano, N. Momono, C. Manabe, Y. Miura, M. Oda and M. Ido, Magnetic susceptibility of superconducting $\text{La}_{2-x}\text{Sr}_x\text{CuO}_4$, *Czech J. Phys.* **46**, 1153 (1996).
- [65] J. W. Loram, K. A. Mirza, W. Y. Liang, J. Osborne, A systematic study of the specific heat anomaly in $\text{La}_{2-x}\text{Sr}_x\text{CuO}_4$, *Physica C* **162–164**, 498 (1989).
- [66] N. Momono, M. Ido, T. Nakano, M. Oda, Y. Okajima, K. Yamaya, Low-temperature electronic specific heat of $\text{La}_{2-x}\text{Sr}_x\text{CuO}_4$ and $\text{La}_{2-x}\text{Sr}_x\text{Cu}_{1-y}\text{Zn}_y\text{CuO}_4$. Evidence for a d wave superconductor, *Physica C* **233**, 395 (1994).
- [67] S. Wakimoto, H. Zhang, K. Yamada, I. Swainson, Hyun-kyung Kim, and R. J. Birgeneau, Direct Relation between the Low-Energy Spin Excitations and Superconductivity of Overdoped High- T_c Superconductors, *Phys. Rev. Lett.* **92**, 217004 (2004).
- [68] S. Wakimoto, K. Yamada, J. M. Tranquada, C. D. Frost, R. J. Birgeneau, and H. Zhang, Disappearance of Antiferromagnetic Spin Excitations in Overdoped $\text{La}_{2-x}\text{Sr}_x\text{CuO}_4$, *Phys. Rev. Lett.* **9**, 247003 (2007).
- [69] M. P. M. Dean, G. Dellea, R. S. Springell, F. Yakhou-Harris, K. Kummer, N. B. Brookes, X. Liu, Y.-J. Sun, J. Strle, T. Schmitt, L. Braicovich, G. Ghiringhelli, I. Bovžović and J. P. Hill, Persistence of magnetic excita-

- tions in $\text{La}_{2-x}\text{Sr}_x\text{CuO}_4$ from the undoped insulator to the heavily overdoped non-superconducting metal, *Nature Materials* **12**, 1019 (2013).
- [70] E. C. Marino, Reginaldo O Corrêa Jr, R. Arouca, Lizardo H. C. M. Nunes and Van Sérgio Alves, Superconducting and pseudogap transition temperatures in high- T_c cuprates and the T_c dependence on pressure, *Supercond. Sci. Technol.* **33**, 035009 (2020).
- [71] R Arouca and E. C. Marino, The resistivity of high- T_c cuprates, *Supercond. Sci. Technol.* **34**, 035004 (2021).
- [72] E. C. Marino and R Arouca, Magnetic field effects on the transport properties of high- T_c cuprates, *Supercond. Sci. Technol.* **34**, 085008 (2021).
- [73] O. Cyr-Choinière, R. Daou, F. Laliberté, C. Collignon, S. Badoux, D. LeBoeuf, J. Chang, B. J. Ramshaw, D. A. Bonn, W. N. Hardy, R. Liang, J.-Q. Yan, J.-G. Cheng, J.-S. Zhou, J. B. Goodenough, S. Pyon, T. Takayama, H. Takagi, N. Doiron-Leyraud, and Louis Taillefer, Pseudogap temperature T^* of cuprate superconductors from the Nernst effect, *Phys. Rev. B* **97**, 064502 (2018).
- [74] R. J. Birgeneau, D. R. Gabbe, H. P. Jenssen, M. A. Kastner, P. J. Picone, T. R. Thurston, G. Shirane, Y. Endoh, M. Sato, K. Yamada, Y. Hidaka, M. Oda, Y. Enomoto, M. Suzuki, and T. Murakami, Antiferromagnetic spin correlations in insulating, metallic, and superconducting $\text{La}_{2-x}\text{Sr}_x\text{CuO}_4$, *Phys. Rev. B* **38**, 6614 (1988);
- [75] S.-D. Chen, M. Hashimoto, Y. He, D. Song, K.-J. Xu, J.-F. He, T.P. Devereaux, H. Eisaki, Dong-Hui Lu, Jan Zaanen, Zhi-Xun Shen, Incoherent strange metal sharply bounded by a critical doping in Bi2212 , *Science* **366**, 1099 (2019).
- [76] M. Le Tacon, M. Minola, D. C. Peets, M. Moretti Sala, S. Blanco-Canosa, V. Hinkov, R. Liang, D. A. Bonn, W. N. Hardy, C. T. Lin, T. Schmitt, L. Braicovich, G. Ghiringhelli, and B. Keimer, Dispersive spin excitations in highly overdoped cuprates revealed by resonant inelastic x-ray scattering, *Phys. Rev. B* **88**, 020501(R) (2013).
- [77] Y. Y. Peng, E. W. Huang, R. Fumagalli, M. Minola, Y. Wang, X. Sun, Y. Ding, K. Kummer, X. J. Zhou, N. B. Brookes, B. Moritz, L. Braicovich, T. P. Devereaux, and G. Ghiringhelli, Dispersion, damping, and intensity of spin excitations in the monolayer $(\text{Bi,Pb})_2(\text{Sr,L a})_2\text{CuO}_{6+\delta}$ cuprate superconductor family, *Phys. Rev. B* **98**, 144507 (2018).